ELSEVIER

1 July 1996

OPTICS COMMUNICATIONS

Optics Communications 128 (1996) 145-157

Full length article

Off-axial pulse propagation in graded-index materials with Kerr nonlinearity – a variational approach

Chih-Hung Chien [a], Shinn-Sheng Yu [a], Yinchieh Lai [a,1], Jyhpyng Wang [b]

[a] *Institute of Electro-Optical Engineering, National Chiao-Tung University, Hsinchu, Taiwan, ROC*

[b] *Institute of Atomic and Molecular Sciences, Academia Sinica and Department of Electrical Engineering, National Taiwan University, Taipei, Taiwan, ROC*

Received 2 January 1996; accepted 5 February 1996

Abstract

We analyze off-axial, self-focused pulse propagation in graded-index Kerr materials with the variational method. Equations which determine the characteristics of the beam, namely the optical path, the wavefront curvature, the beam width, and the pulse duration are derived and solved. We show that continuously adjustable negative group-velocity dispersion can be generated by off-axial propagation, and for pulse energy smaller than a critical value, negative group-velocity dispersion and Kerr nonlinearity warrant the existence of stable spatio-temporal solitary pulses.

1. Introduction

Recently one of the authors (J. Wang) and his associates showed that continuously adjustable negative group-velocity dispersion can be produced by propagating Gaussian beams off the axis of a graded-index material [1,2]. The idea is shown in Fig. 1. This is an interesting and useful discovery because dispersion control has always been an important issue in the generation and application of ultrashort optical pulses and in wavelength multiplexed optical signal processing. Unlike the common dispersion-control methods which use prism-pairs or grating-pairs, graded-index materials take little physical space to produce a large amount of negative group-velocity dispersion and suffer negligible optical loss. Therefore, graded-index materials have a great potential for dispersion control in optical devices, especially in integrated optics.

A graded-index material is a material with a parabolic refractive index distribution given by

$$n(x,y,z,\omega) = n_0(\omega)\left[1 - \tfrac{1}{2}G(\omega)(x^2+y^2)\right], \tag{1}$$

where $G(\omega)$ is the strength of the index gradient. In a graded-index material the group-velocity dispersion caused by the frequency dependence of $G(\omega)$ (the index gradient dispersion) has a sign opposite to the group-velocity dispersion caused by the frequency dependence of $n_0(\omega)$ (the material dispersion, usually positive).

[1] E-mail: yclai@cc.nctu.edu.tw.

PII S0030-4018(96)00128-9

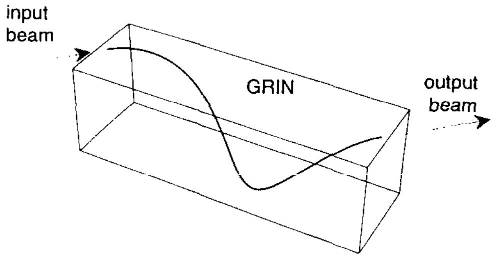

Fig. 1. Schematic of off-axial pulse propagation in a graded-index material.

As shown in Eq. (1), the net effect of the index gradient dispersion is proportional to the square of the offset distance from the beam center to the axis. In addition off-axial propagation also produces negative geometric group-velocity dispersion. Therefore, by adjusting the offset distance, the net group-velocity dispersion can be continuously controlled.

Negative group-velocity dispersion also suggests the existence of optical solitons. In another paper [3], Wang and Chang showed that optical solitons in a broad spectral range can be produced by off-axial propagation in graded-index Kerr materials. However, in that paper the analysis is done in the weak self-focusing limit. It is not clear how self-focusing would affect the stability of these solitons. Nevertheless self-focusing produces stable spatial solitons in two-dimensional homogeneous Kerr materials. In three-dimensional materials self-focusing exhibits collapse phenomena [4]. Because graded-index Kerr materials can be used as novel platforms for applications of optical solitons, it is important to find out whether or not graded-index Kerr materials can support stable spatio-temporal solitons (or solitary pulses) under the combined effect of graded-index, diffraction, self-focusing, group-velocity dispersion, and self-phase modulation. In this paper, we develop a variational approach to study the off-axial pulse propagation problem in graded-index Kerr materials. In the literature, the variational approach based on the Lagrangian formulation and Ritz optimization procedure has been widely applied to the studies of temporal and spatial soliton phenomena [5–9]. On-axial cw propagation in graded-index Kerr materials has also been investigated with such an approach [10,11]. It is found that there exist stable, stationary solutions when the optical power is less than a critical value. This is because graded-index helps counteract diffraction, so that the beam profile can remain stationary below the critical power. Yet it is not clear whether graded-index Kerr materials can support stationary propagation of optical pulses, because unlike a cw beam in which the optical power is constant, in an optical pulse the instantaneous power varies greatly from the pulse peak to the pulse wings. Recently, we have used the same variational approach to study on-axial pulse propagation in graded-index Kerr materials and showed that stable spatio-temporal solitary pulses can exist as long as the net group-velocity dispersion is negative and the pulse energy is less than a critical value [12]. However, to obtain negative group-velocity dispersion in the spectral range where the material dispersion is positive, off-axial propagation is required [3]. This calls for an extensive study on off-axial, nonlinear pulse propagation problems. In particular, for off-axial propagation the commonly used paraxial approximation needs to be examined carefully. Moreover, the Kerr nonlinearity and the rapidly varying intensity of optical pulses further increase the complexity of the problem. We find that the variational method is an elegant approach to the analytical complexity described above. With an appropriate solution ansatz, the variational method reveals the general behavior of Gaussian beam propagation in graded-index Kerr materials and displays the interaction between effects of refraction, diffraction, self-focusing, group-velocity dispersion, and self-phase modulation in a unified formalism.

The paper is organized as follows. In Section 2, using the operator expansion technique, we start from the wave equation in the frequency domain to derive the off-axial pulse propagation equation in graded-index materials. In Section 3, we study the linear pulse propagation problem using the variational method. The pulse shape in space is assumed to be Gaussian and the pulse shape in time is assumed to be a hyperbolic secant. The evolution equations of the pulse parameters are derived. From these evolution equations, the contributions to the net group-velocity dispersion are identified and their analytic expressions are given. In Section 4, we improve the estimation of the net group-velocity dispersion by including higher order terms in the operator expansion. It is found that the paraxial wave equation underestimates the net group-velocity dispersion when the offset distance is large. Adjustable negative group-velocity dispersion up to 936 fs^2 can be generated by using a 1 cm long commercially available graded-index material at 800 nm. In Section 5, with the Kerr nonlinearity included in the formulation, we show that stable spatio-temporal solitary pulses can exist and the criteria of existence are derived. The conclusions are backed up with numerical simulations.

2. Off-axial pulse propagation in graded-index materials

In the frequency domain, the scalar wave equation in a graded-index material with a parabolic refractive index given in Eq. (1) can be written as

$$\left(\frac{\partial^2}{\partial z^2} + \nabla_T^2 + k^2(\omega)[1 - \tfrac{1}{2}G(\omega)r^2]^2\right) E(x,y,z,\omega) = 0. \tag{2}$$

Here $r^2 = x^2 + y^2$, ∇_T^2 is the transverse Laplacian operator, and

$$k(\omega) = n_0(\omega)\omega/c. \tag{3}$$

Eq. (2) is a second order partial differential equation in z. However, if the light field propagates only in the $+z$ direction, then Eq. (2) can be formally reduced to a first order partial differential equation in z as shown in the following equation:

$$\partial E/\partial z = i[k^2(1 - \tfrac{1}{2}Gr^2)^2 + \nabla_T^2]^{1/2}E. \tag{4}$$

The meaning of the square root of the operator in Eq. (4) has to be understood as its Taylor's expansion.

If the propagation direction is close to the z-axis, then it is advantageous to write

$$E(x,y,z,\omega) = \tilde{u}(x,y,z,\omega)\, e^{ik_0 z} \tag{5}$$

and to derive an evolution equation for $\tilde{u}(x,y,z,\omega)$ instead of $E(x,y,z,\omega)$. Here $k_0 = k(\omega_0)$ is the propagation constant and ω_0 is the carrier frequency.

By substituting Eq. (5) into Eq. (4) and carrying out the expansion to first order in r^2 and ∇_T^2, we obtain

$$\frac{\partial \tilde{u}}{\partial z} = i(k - k_0)\tilde{u} + ik\left(-\tfrac{1}{2}Gr^2 + \frac{1}{2k^2}\nabla_T^2\right)\tilde{u}. \tag{6}$$

Eq. (6) is the paraxial wave equation in the frequency domain. We shall use it as our starting point to study the problem and check its validity in Section 4.

To derive the propagation equation in the time domain, we expand the frequency dependent terms k and G in Eq. (6) around the carrier frequency ω_0 up to second order, then perform the inverse Fourier transform. We obtain the following equation,

$$i\frac{\partial u}{\partial z} = -id_1\frac{\partial u}{\partial t} + \frac{d_2}{2}\frac{\partial^2 u}{\partial t^2} + r^2\left(\beta_0 + i\beta_1\frac{\partial}{\partial t} - \frac{\beta_2}{2}\frac{\partial^2}{\partial t^2}\right)u + \left(-\alpha_0 - i\alpha_1\frac{\partial}{\partial t} + \frac{\alpha_2}{2}\frac{\partial^2}{\partial t^2}\right)\nabla_T^2 u. \tag{7}$$

Here $u(x,y,z,t)$ is the pulse envelope in the time domain. The coefficients in Eq. (7) are given by

$$d_1 = (\mathrm{d}/\mathrm{d}\omega)k, \tag{8}$$

$$d_2 = (\mathrm{d}^2/\mathrm{d}\omega^2)k, \tag{9}$$

$$\beta_0 = \tfrac{1}{2}k_0G_0, \tag{10}$$

$$\beta_1 = (\mathrm{d}/\mathrm{d}\omega)(\tfrac{1}{2}kG), \tag{11}$$

$$\beta_2 = (\mathrm{d}^2/\mathrm{d}\omega^2)(\tfrac{1}{2}kG), \tag{12}$$

$$\alpha_0 = 1/2k_0, \tag{13}$$

$$\alpha_1 = (\mathrm{d}/\mathrm{d}\omega)(1/2k), \tag{14}$$

$$\alpha_2 = (\mathrm{d}^2/\mathrm{d}\omega^2)(1/2k). \tag{15}$$

Here $k_0 = k(\omega_0)$, $G_0 = G(\omega_0)$, and all the derivatives are evaluated at $\omega = \omega_0$.

Eq. (7) is the pulse propagation equation in the time domain. It differs from the usually used on-axis paraxial pulse propagation equation, in which $d_1 = \beta_1 = \beta_2 = \alpha_1 = \alpha_2 = 0$. Among these additional terms, the important ones are $\alpha_2\, \partial^2/\partial t^2\, \nabla_T^2 u$ and $\beta_2 r^2\, \partial^2/\partial t^2\, u$. As we shall see, these two terms give rise to the negative geometric group-velocity dispersion.

3. Variational formulation of linear pulse propagation

It is very difficult to find exact analytical solutions to Eq. (7). Direct numerical simulation is also not feasible because Eq. (7) is a four-dimensional partial differential equation. Our approximate analytical method is based on the variational technique that has been used successfully for studying soliton phenomena. The starting point is to reformulate the problem variationally.

It is not difficult to show that Eq. (7) is equivalent to the following variational equation,

$$\delta \iiiint L\,\mathrm{d}x\,\mathrm{d}y\,\mathrm{d}z\,\mathrm{d}t = 0. \tag{16}$$

Here the Lagrangian density L is given by

$$\begin{aligned} L = {}& \frac{1}{2}i\left(u^*\frac{\partial u}{\partial z} - \frac{\partial u^*}{\partial z}u\right) + \frac{d_1}{2}i\left(u^*\frac{\partial u}{\partial t} - \frac{\partial u^*}{\partial t}u\right) + \frac{d_2}{2}\left|\frac{\partial u}{\partial t}\right|^2 \\ & -\beta_0 r^2|u|^2 - \frac{\beta_1}{2}r^2 i\left(u^*\frac{\partial u}{\partial t} - \frac{\partial u^*}{\partial t}u\right) - \frac{\beta_2}{2}r^2\left|\frac{\partial u}{\partial t}\right|^2 \\ & -\alpha_0\,|\nabla_T u|^2 - \frac{\alpha_1}{2}i\left(\nabla_T u^*\cdot\frac{\partial \nabla_T u}{\partial t} - \frac{\partial \nabla_T u^*}{\partial t}\cdot\nabla_T u\right) - \frac{\alpha_2}{2}\left|\frac{\partial \nabla_T u}{\partial t}\right|^2, \end{aligned} \tag{17}$$

where ∇_T is the transverse gradient operator. The power of the variational method is that one can use a much simpler trial function to approximate the real solution and get sufficiently accurate results. For our problem, we will assume that the pulse envelope $u(x, y, z, t)$ can be well approximated by the following trial function,

$$
\begin{aligned}
u(x,y,z,t) = {} & A(z)\exp[i\theta(z)]\exp\left(-\frac{[x-x_0(z)]^2}{2w_x^2(z)}\right)\exp\left(-\frac{(y-y_0(z))^2}{2w_y^2(z)}\right)\operatorname{sech}\left(\frac{t-t_0(z)}{w_t(z)}\right) \\
& \times\exp\{\tfrac{1}{2}ip_x(z)[x-x_0(z)]^2+ik_x(z)[x-x_0(z)]\} \\
& \times\exp\{\tfrac{1}{2}ip_y(z)[y-y_0(z)]^2+ik_y(z)[y-y_0(z)]\} \\
& \times\exp\{-\tfrac{1}{2}ip_t(z)[t-t_0(z)]^2\}.
\end{aligned} \tag{18}
$$

Here the pulse envelope $u(x,y,z,t)$ is assumed to be separable in the x, y, t dimensions. x_0, y_0 are the transverse coordinates of the pulse center, k_x, k_y are the transverse components of the pulse propagation wave vector, w_x, w_y are the transverse spatial beam widths. p_x, p_y are the wavefront curvatures, t_0 is the time-position of the pulse center, w_t is the pulse duration, and p_t is the temporal chirp of the pulse. All these variables are functions of the propagation distance z. The pulse shape in space is assumed to be Gaussian and the pulse shape in time is assumed to be a hyperbolic secant. Different assumptions of the pulse shape will only cause a difference in the parameters of the Euler equations derived from the Lagrangian density. Inserting the trial solution (18) into the variational equation (16) and carrying out the integration over x, y, and z, one obtains the following reduced variational equation,

$$\delta\int\langle L\rangle\,\mathrm{d}z = 0. \tag{19}$$

Here the reduced Lagrangian density $\langle L\rangle$ is given by

$$
\begin{aligned}
\langle L\rangle = {} & 2\pi A^2 w_x w_y w_t S, \\
S = {} & -\frac{\mathrm{d}\theta}{\mathrm{d}z}+k_x\frac{\mathrm{d}x_0}{\mathrm{d}z}+k_y\frac{\mathrm{d}y_0}{\mathrm{d}z}-\frac{1}{4}\left(w_x^2\frac{\mathrm{d}p_x}{\mathrm{d}z}+w_y^2\frac{\mathrm{d}p_y}{\mathrm{d}z}\right)+\frac{\pi^2}{24}w_t^2\frac{\mathrm{d}p_t}{\mathrm{d}z} \\
& +d_2\left(\frac{1}{6}\frac{1}{w_t^2}+\frac{\pi^2}{24}w_t^2p_t^2\right)-\beta_0[(x_0^2+y_0^2)+\tfrac{1}{2}(w_x^2+w_y^2)] \\
& -\beta_2\left(\frac{1}{6}\frac{1}{w_t^2}+\frac{\pi^2}{24}w_t^2p_t^2\right)[(x_0^2+y_0^2)+\tfrac{1}{2}(w_x^2+w_y^2)] \\
& -\alpha_0\left[(k_x^2+k_y^2)+\frac{1}{2}\left(\frac{1}{w_x^2}+\frac{1}{w_y^2}\right)+\tfrac{1}{2}(w_x^2p_x^2+w_y^2p_y^2)\right] \\
& -\alpha_2\left(\frac{1}{6}\frac{1}{w_t^2}+\frac{\pi^2}{24}w_t^2p_t^2\right)\left[(k_x^2+k_y^2)+\frac{1}{2}\left(\frac{1}{w_x^2}+\frac{1}{w_y^2}\right)+\tfrac{1}{2}(w_x^2p_x^2+w_y^2p_y^2)\right].
\end{aligned} \tag{20}
$$

The Euler equations of Eq. (19) are a set of coupled ordinary differential equations for the pulse function parameters which together describe the propagation of the pulse. These evolution equations of A, x_0, k_x, w_x, p_x, w_t, and p_t are given below:

$$A^2 w_x w_y w_t = \text{const} \equiv E_p/2\pi, \tag{21}$$

$$\frac{\mathrm{d}x_0}{\mathrm{d}z} = 2\left[\alpha_0+\alpha_2\left(\frac{1}{6}\frac{1}{w_t^2}+\frac{\pi^2}{24}w_t^2p_t^2\right)\right]k_x, \tag{22}$$

$$\frac{dk_x}{dz} = -2\left[\beta_0 + \beta 2\left(\frac{1}{6}\frac{1}{w_t^2} + \frac{\pi^2}{24}w_t^2 p_t^2\right)\right] x_0, \tag{23}$$

$$\frac{dw_x}{dz} = 2\left[\alpha_0 + \alpha_2\left(\frac{1}{6}\frac{1}{w_t^2} + \frac{\pi^2}{24}w_t^2 p_t^2\right)\right] w_x p_x, \tag{24}$$

$$\frac{dp_x}{dz} = 2\left[\alpha_0 + \alpha_2\left(\frac{1}{6}\frac{1}{w_t^2} + \frac{\pi^2}{24}w_t^2 p_t^2\right)\right]\left(\frac{1}{w_x^4} - p_x^2\right) - 2\left[\beta_0 + \beta_2\left(\frac{1}{6}\frac{1}{w_t^2} + \frac{\pi^2}{24}w_t^2 p_t^2\right)\right], \tag{25}$$

$$dw_t/dz = (d_2 - \alpha_2 J_1 - \beta_2 J_2) w_t p_t, \tag{26}$$

$$\frac{dp_t}{dz} = (d_2 - \alpha_2 J_1 - \beta_2 J_2)\left(\frac{4}{\pi^2}\frac{1}{w_t^4} - p_t^2\right). \tag{27}$$

The equations for y_0, k_y, w_y, and p_y are of the same form as those for x_0, k_x, w_x, and p_x. Evolution equations for t_0 and θ are not shown here since they are not important for our discussion. In Eq. (21), E_p is the pulse energy. In Eqs. (26) and (27), J_1 and J_2 are defined according to

$$J_1 = \frac{1}{2}\left(\frac{1}{w_x^2} + \frac{1}{w_y^2}\right) + \tfrac{1}{2}(w_x^2 p_x^2 + w_y^2 p_y^2) + (k_x^2 + k_y^2), \tag{28}$$

$$J_2 = \tfrac{1}{2}(w_x^2 + w_y^2) + (x_0^2 + y_0^2). \tag{29}$$

Consider a typical graded-index material, SML-W2.0 GRIN rod (Selfoc Micro Lens-W type of 2.0 mm diameter from NSG America Inc.), the wavelength dependence of n_0 is given by

$$n_0(\lambda) = 1.5868 + 8.14 \times 10^{-3}/\lambda^2, \tag{30}$$

and the wavelength dependence of G is given by

$$G(\lambda) = (0.2931 + 2.369 \times 10^{-3}/\lambda^2 + 7.681 \times 10^{-4}/\lambda^4)^2\ \mathrm{mm}^{-2}. \tag{31}$$

Here λ is the wavelength in units of μm. From the formula given above, at the 800 nm wavelength, one has $d_2 = 1.08 \times 10^{-25}$ s^2/m, $\beta_0 = 5.60 \times 10^{11}$ m^{-3}, $\beta_2 = 4.61 \times 10^{-20}$ s^2/m^3, $\alpha_0 = 3.98 \times 10^{-8}$ m, and $\alpha_2 = 1.45 \times 10^{-38}$ m s^2. These are the typical parameters for commercially available graded-index materials. Given these values, it is safe to make the following two approximations

$$\alpha_2\left(\frac{1}{6}\frac{1}{w_t^2} + \frac{\pi^2}{24}w_t^2 p_t^2\right) \ll \alpha_0, \tag{32}$$

$$\beta_2\left(\frac{1}{6}\frac{1}{w_t^2} + \frac{\pi^2}{24}w_t^2 p_t^2\right) \ll \beta_0. \tag{33}$$

These two approximations should be valid even if w_t is of the order of several femtoseconds.

With the above two approximations, Eqs. (21)–(27) are much simplified.

$$A^2 w_x w_y w_t = \mathrm{const} \equiv E_p/2\pi, \tag{34}$$

$$dx_0/dz = 2\alpha_0 k_x, \tag{35}$$

$$dk_x/dz = -2\beta_0 x_0, \tag{36}$$

$$dw_x/dz = 2\alpha_0 w_x p_x, \tag{37}$$

$$dp_x/dz = 2\alpha_0(1/w_x^4 - p_x^2) - 2\beta_0, \tag{38}$$

$$\mathrm{d}w_t/\mathrm{d}z = (d_2 - \alpha_2 J_1 - \beta_2 J_2) w_t p_t, \tag{39}$$

$$\frac{\mathrm{d}p_t}{\mathrm{d}z} = (d_2 - \alpha_2 J_1 - \beta_2 J_2)\left(\frac{4}{\pi^2}\frac{1}{w_t^4} - p_t^2\right). \tag{40}$$

Eqs. (34)–(40) have the following interesting characteristics:

(i) Eq. (34) is the pulse energy conservation equation.

(ii) x_0 and k_x are coupled together in the same way as in the case of a cw Gaussian beam propagating off-axially through the graded-index waveguide. The evolution of x_0 and k_x are independent of the evolution of other parameters. The solutions are periodic functions given by

$$x_0(z) = a_x \sin(\sqrt{4\alpha_0\beta_0}\, z + \phi_x), \tag{41}$$

$$k_x(z) = \sqrt{\beta_0/\alpha_0}\, a_x \cos(\sqrt{4\alpha_0\beta_0}\, z + \phi_x). \tag{42}$$

Here a_x and ϕ_x are constants to be determined from the initial conditions.

(iii) Similarly, the evolution of y_0 and k_y are given by

$$y_0(z) = a_y \sin(\sqrt{4\alpha_0\beta_0}\, z + \phi_y), \tag{43}$$

$$k_y(z) = \sqrt{\beta_0/\alpha_0} \cos(\sqrt{4\alpha_0\beta_0}\, z + \phi_y). \tag{44}$$

If we choose the initial condition to be $a_x = a_y = a$, $\phi_x = \pi/2$, $\phi_y = 0$, then $x_0^2(z) + y_0^2(z) = \text{const} = a^2$ and $k_x^2 + k_y^2 = \text{const} = (\beta_0/\alpha_0)a^2$. That is, the pulse propagates in a helix trajectory. In this case, the offset distance is constant.

(iv) The difference between on-axial and off-axial pulse propagation does not show up in the evolution equations of w_x and p_x. The parameters w_x and p_x are coupled together in the same way as in the case of a cw Gaussian beam propagating axially through the graded-index waveguide. Parameters w_t and p_t do not appear in the equations of w_x and p_x. This implies the temporal evolution does not affect the spatial evolution. The inverse is not true.

(v) There exists a stationary solution of w_x and p_x such that $p_x(z) = 0$ and

$$w_x(z) = \text{const} = (\alpha_0/\beta_0)^{1/4}. \tag{45}$$

This is called the stationary beam width of a graded-index material.

(vi) The difference between on-axial and off-axial pulse propagation appears in the evolution equations of w_t and p_t. The net dispersion parameter is given by

$$D \equiv d_2 - \alpha_2 J_1 - \beta_2 J_2, \tag{46}$$

with J_1 and J_2 given in Eqs. (28), (29). There are three contributions to the net group-velocity dispersion. The first term is the material dispersion due to the frequency dependence of n_0. The second term is the geometric group-velocity dispersion due to off-axial propagation. The third term is the material dispersion due to the frequency dependence of G and off-axial propagation. For typical graded-index materials, α_2 and β_2 are all positive.

(vii) If the initial beam width $w_x(0)$, $w_y(0)$ is set equal to the stationary beam width according to Eq. (45) and the pulse propagates in a helix trajectory, then J_1 and J_2 can be well approximated by

$$J_1(z) \approx \text{const} = (\beta_0/\alpha_0)a^2, \tag{47}$$

$$J_2(z) \approx \text{const} = a^2, \tag{48}$$

when the offset distance a is much larger than the beam width. In this special case, the net dispersion parameter is a constant given by

$$D \equiv d_2 - \alpha_2(\beta_0/\alpha_0)a^2 - \beta_2 a^2. \tag{49}$$

Thus the net dispersion parameter can be made negative by choosing a sufficiently large offset distance a.

(viii) Up to this point, we have derived an expression for the net group-velocity dispersion parameter by assuming the beam width is equal to the stationary beam width and the pulse propagates in a helix trajectory. The dispersion parameter is constant in this special case. In general situations, since the offset distance, the beam width, and the propagation direction are periodic functions of the propagation distance, the net dispersion parameter is a also a periodic function of the propagation distance.

4. Net group-velocity dispersion

Expression (49) for the net dispersion parameter is based on the paraxial approximation in the frequency domain, Eq. (7). In this section we will check its accuracy by comparing it with a more accurate estimation.

Let us take a look at the exact wave equation, Eq. (4), again. If we rewrite it as

$$\frac{\partial E}{\partial z} = i\{k^2(\omega)[1 - \tfrac{1}{2}G(\omega)r^2]^2 + \nabla_T^2\}^{1/2}E \equiv i\beta(\omega)E, \tag{50}$$

then at least formally the group-velocity dispersion parameter is given by

$$D = \frac{\partial^2\beta}{\partial\omega^2} = \frac{\partial^2}{\partial\omega^2}\{k^2(\omega)[1 - \tfrac{1}{2}G(\omega)r^2]^2 + \nabla_T^2\}^{1/2}. \tag{51}$$

Eq. (51) is just a formal expression. However, in the previous section, we mentioned that the spatial and temporal pulse evolution can be decoupled. We also assume that the spatial evolution of the pulse is roughly the same as that predicted by the paraxial wave equation. The validity of this assumption has been checked by estimating the magnitudes of higher order terms that affect spatial evolution. In the limit that the beam width is much smaller than the beam offset, it is found that the net correction due to higher order terms is less than 1% when the offset distance is 1 mm (the radius of the SML-W2.0 GRIN rod). When the offset distance is smaller, the net correction is even smaller. Therefore it is safe to assume that the spatial evolution of the pulse is the same as that described by the paraxial wave equation. With these observations, we find that, in the limit that the beam width is much smaller than the beam offset, one can safely replace the operator ∇_T^2 with $-(k_x^2 + k_y^2)$ in Eq. (51). If the pulse propagates in a helix trajectory, then one has $r^2 = a^2$ and $k_x^2 + k_y^2 = (\beta_0/\alpha_0)a^2$. In this case, the net dispersion parameter is given by

$$D = \frac{\partial^2}{\partial\omega^2}\{k^2(\omega)[1 - \tfrac{1}{2}G(\omega)a^2]^2 - (\beta_0/\alpha_0)a^2\}^{1/2}. \tag{52}$$

Eq. (52) is a more accurate estimation of the net dispersion parameter since it includes all higher order terms in the operator expansion. Using the SML-W2.0 GRIN rod mentioned in the previous section as a numerical example again, we calculate the dispersion parameter at 800 nm for three offset distances. Results from Eq. (49) and the more accurate Eq. (52) are tabulated together in Table 1 for comparison. It can be seen that when the offset distance is small, the material dispersion dominates and the net dispersion parameter is positive. However, when the offset distance is sufficiently large, the net dispersion parameter becomes negative. It can also be seen that when the offset distance is small, predictions from Eq. (49) and Eq. (52) do not differ very much. However, when the offset distance is 1 mm, the radius of the SML-W2.0 GRIN rod, the prediction from Eq. (52) is 1.35 times larger than that from Eq. (49). The half-pitch length of this graded-index lens is $\pi/2\sqrt{\alpha_0\beta_0} = 1.05$ cm. Therefore the net negative dispersion generated by off-axial propagation through a

Table 1
Dispersion parameters (in fs^2/mm) for different beam offsets. Estimation is based on the data of SML-W2.0 GRIN rod at the 800 nm wavelength

Beam offset distance	0.5 mm	0.75 mm	1.0 mm
Material dispersion: d_2	108	108	108
Geometric dispersion: $-\alpha_2(\beta_0/\alpha_0)a^2$	−51.0	−115	−204
Graded index dispersion: $-\beta_2 a^2$	−11.5	−25.9	−46.1
D from Eq. (49)	45.6	−32.4	−142
D from Eq. (52)	43.2	−45.5	−187

half-pitch SML-W2.0 GRIN rod can be as large as 1970 fs^2 when the offset distance is equal to the radius of the graded-index lens. This equals the positive dispersion of 3.39 cm of sapphire. In principle, one may increase G or the radius of the graded-index lens to produce even larger negative dispersion. But in fact, the radius of a graded-index lens is limited by the maximum refractive index change that can be made. For commercial glass graded-index lenses the index drop from the center to the edge is about 0.05.

One may wonder why Eq. (7) gives a poor description of the dispersion parameter (or the temporal evolution) while its description of the spatial evolution is sufficiently accurate. This is because even if $1+\frac{1}{2}x$ is a good approximation to $\sqrt{1+x}$, $1+\frac{1}{2}\partial^2 x/\partial\omega^2$ may not be a good approximation to $\partial^2\sqrt{1+x}/\partial\omega^2$. It is just because the spatial evolution described by Eq. (7) is sufficiently accurate in the case studied here, that we are able to derive the more accurate expression Eq. (52) for the net dispersion parameter.

5. Nonlinear pulse propagation and stable spatio-temporal solitary pulses

In this section we study the pulse propagation problem in nonlinear graded-index materials. Including Kerr nonlinearity in the formulation, the paraxial wave equation in the time domain becomes

$$\begin{aligned}\frac{\partial u}{\partial z} &= -d_1\frac{\partial u}{\partial t} - i\frac{d_2}{2}\frac{\partial^2 u}{\partial t^2} + r^2\left(-i\beta_0 + \beta_1\frac{\partial}{\partial t} + i\frac{\beta_2}{2}\frac{\partial^2}{\partial t^2}\right)u \\ &\quad + \left(i\alpha_0 - \alpha_1\frac{\partial}{\partial t} - i\frac{\alpha_2}{2}\frac{\partial^2}{\partial t^2}\right)\nabla_T^2 u + iK|u|^2 u.\end{aligned} \tag{53}$$

The term containing K is the contribution of the Kerr nonlinearity and the constant K is defined by

$$K = \frac{k(\omega_0)n_2}{n_0(\omega_0)}. \tag{54}$$

Here n_2 is the nonlinear coefficient of the refractive index.

The Lagrangian density with Kerr nonlinearity is the same as Eq. (17) except an additional term, $\frac{1}{2}K|u|^4$. The evolution equations of x_0, and k_x are exactly the same as Eqs. (22), (23). The evolution equations of w_x, p_x, w_t and p_t are now

$$\mathrm{d}w_x/\mathrm{d}z = 2\alpha_0 w_x p_x, \tag{55}$$

$$\frac{\mathrm{d}p_x}{\mathrm{d}z} = 2\alpha_0\left(\frac{1}{w_x^4} - p_x^2\right) - 2\beta_0 - \frac{KE_p}{6\pi w_x^3 w_y w_t}, \tag{56}$$

$$\mathrm{d}w_t/\mathrm{d}z = Dw_t p_t, \tag{57}$$

$$\frac{\mathrm{d}p_t}{\mathrm{d}z} = D\left(\frac{4}{\pi^2}\frac{1}{w_t^4} - p_t^2\right) + \frac{KE_p}{\pi^3 w_x w_y w_t^3}. \tag{58}$$

Here D is the net dispersion parameter defined in Eq. (46). The evolution equations for pulse parameters in the y dimension are similar. It is interesting to note that Eqs. (55)-(58) still hold if the pulse propagates on-axially. The only difference is that $D = d_2$ for on-axial propagation. Therefore, the following derivation is similar to our recent study on on-axial solitary pulse propagation [12].

In the following we shall consider a special case where

(i) The beam is circular ($w_x = w_y = w$ and $p_x = p_y = p$).

(ii) The beam width is much smaller than the offset distance.

(iii) The beam propagates in a helix trajectory such that the offset distance is constant.

(iv) From item (ii) and (iii), the net dispersion parameter D is constant. We will also assume that it is negative ($D = -|D|$).

By introducing normalized quantities, the equations become

$$\mathrm{d}\bar{w}/\mathrm{d}\bar{z} = 2\bar{w}\bar{p}, \tag{59}$$

$$\frac{\mathrm{d}\bar{p}}{\mathrm{d}\bar{z}} = 2\left(\frac{1}{\bar{w}^4} - \bar{p}^2\right) - 2 - \frac{\bar{E}_p}{6\pi\bar{w}^4\bar{w}_t}, \tag{60}$$

$$\mathrm{d}\bar{w}_t/\mathrm{d}\bar{z} = -\bar{w}_t\bar{p}_t, \tag{61}$$

$$\frac{\mathrm{d}\bar{p}_t}{\mathrm{d}\bar{z}} = -\left(\frac{4}{\pi^2}\frac{1}{\bar{w}_t^4} - \bar{p}_t^2\right) + \frac{\bar{E}_p}{\pi^3\bar{w}^2\bar{w}_t^3}. \tag{62}$$

Here $\bar{z}$, $\bar{w}$, $\bar{w}_t$, and $\bar{E}_p$ are dimensionless normalized quantities and the normalization units are (a) propagation distance: $z_N = (\alpha_0\beta_0)^{-1/2}$; (b) beam width: $w_N = (\alpha_0/\beta_0)^{1/4}$; (c) pulse duration: $w_{tN} = (|D|/\sqrt{\alpha_0\beta_0})^{1/2}$; (d) intensity: $I_N = \sqrt{\alpha_0\beta_0}/K$; (e) pulse energy: $E_{pN} = I_N w_N^2 w_{tN}$.

Eqs. (59)-(62) describe the dynamic interplay among the dispersion, diffraction, graded-index effect, and nonlinearity. The stationary solutions that satisfy

$$\mathrm{d}\bar{w}/\mathrm{d}\bar{z} = \mathrm{d}\bar{p}/\mathrm{d}\bar{z} = \mathrm{d}\bar{w}_t/\mathrm{d}\bar{z} = \mathrm{d}\bar{p}_t/\mathrm{d}\bar{z} = 0 \tag{63}$$

are given by

$$\bar{p} = \bar{p}_t = 0, \tag{64}$$

$$\bar{w}_t = (4\pi/\bar{E}_p)\bar{w}^2, \tag{65}$$

$$(\bar{w}^2)^3 - (\bar{w}^2) + \bar{E}_p^2/48\pi^2 = 0. \tag{66}$$

Eq. (66) is a third order polynomial equation in $\bar{w}^2$. To have meaningful solutions ($\bar{w}^2 > 0$), Eq. (66) needs to have positive real roots. The condition for Eq. (66) to have positive real roots is given by

$$\bar{E}_p \le 2^{5/2}3^{-1/4}\pi \approx 13.5034. \tag{67}$$

Thus the normalized critical energy is $2^{5/2} \times 3^{-1/4}\pi$.

With any given $\bar{E}_p$ that satisfies Eq. (67), Eqs. (59)-(62) have two stationary solutions. The normalized stationary beam width and pulse duration are plotted in Figs. 2 and 3, respectively. After linearizing Eqs. (59)-(62) near the stationary solutions and examining the eigensolutions of the linearized equations, we find that only the upper branch of the solution is stable.

Eq. (67) and $D < 0$ are the existence criteria of stable spatio-temporal solitary pulses in a graded-index waveguide with Kerr nonlinearity. It should be noted that if $\beta_0 = 0$ (no graded index), then Eq. (66) reduces

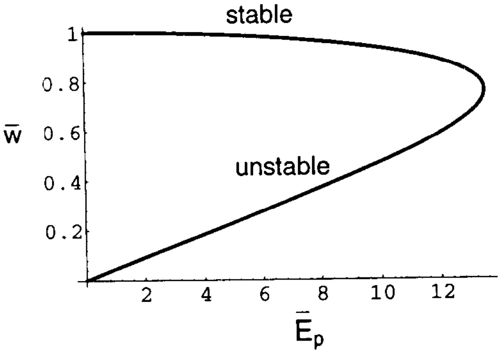

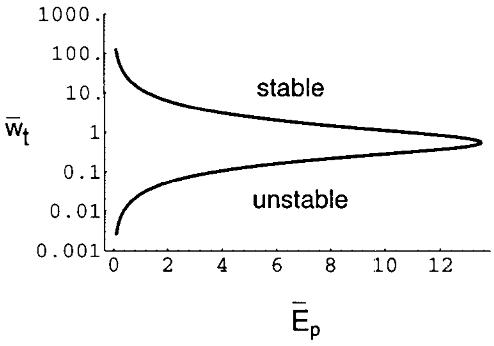

Fig. 2. Normalized beam width versus normalized pulse energy of the solitary pulses.

Fig. 3. Normalized pulse duration versus normalized pulse energy of the solitary pulses.

to a first order polynomial equation in $\bar{w}^2$. The solution is thus not stable. This reproduces the well-known result that spatio-temporal solitary pulses are not stable in a homogeneous Kerr medium.

For the SML-W2.0 GRIN rod, at the 800 nm wavelength, we have seen in the previous sections that $d_2 = 1.08 \times 10^{-25}$ s^2/m, $\beta_0 = 5.60 \times 10^{11}$ m^{-3}, $\beta_2 = 4.61 \times 10^{-20}$ s^2/m^3, $\alpha_0 = 3.98 \times 10^{-8}$ m, and $\alpha_2 = 1.45 \times 10^{-38}$ m s^2. Let us now assume a nonlinear coefficient, $n_2 = 3.20 \times 10^{-20}$ m^2/W, the value of fused silica, then $K = 2.51 \times 10^{-13}$ m/W. When the net dispersion parameter D is written as $-d \times 10^{-25}$ s^2/m, the normalization units are (a) propagation distance: $z_N = 6.70$ mm; (b) beam width: $w_N = 16.3$ μm; (c) pulse duration: $w_{tN} = 25.9 \times \sqrt{d}$ fs; (d) pulse energy: $E_{pN} = 4.10 \times \sqrt{d}$ nJ. For the SML-W2.0 GRIN rod, d varies from -1.08 to 1.87, as can be seen in Table 1.

These values show that it is not difficult to generate spatio-temporal solitary pulses in graded-index materials with ordinary ultrashort pulse lasers. For on-axial solitary pulse propagation, the predictions from the variational method have been verified by direct numerical simulation of the paraxial wave equation [12]. The result of the numerical simulation strongly supports the validity of the variational approach employed here. Under the normalization units used, the paraxial wave equation for on-axial propagation is

$$\frac{\partial \bar{u}}{\partial \bar{z}} = i\left(\frac{\partial^2 \bar{u}}{\partial \bar{x}^2} + \frac{\partial^2 \bar{u}}{\partial \bar{y}^2}\right) + i\frac{1}{2}\frac{\partial^2 \bar{u}}{\partial \bar{t}^2} - i(\bar{x}^2 + \bar{y}^2)\bar{u} + i|\bar{u}|^2\bar{u}. \tag{68}$$

We take advantage of the cylindrical symmetry to reduce the computational complexity by one dimension and use the finite difference beam propagation method [13] to propagate the pulse. Our finite difference beam propagation method is based on the Crank-Nicholson method [14] and we use five-point finite difference formula in the temporal and transverse spatial dimension. Since Eq. (74) is nonlinear, an iterative procedure is implemented to insure the accuracy of each propagation step. The solitary pulse solution from the variational analysis is used as the initial condition. We have calculated the peak amplitude, pulse duration, and beam width for solitary pulses with the normalized pulse energy $\bar{E}_p$ equal to 2, 4, 6, 8, 10, 12. The pulse parameters for $\bar{E}_p = 6$ are shown in Fig. 4. The evolutions of spatial and temporal pulse shapes are shown in Figs. 5 and 6. The initial conditions are $\bar{A} = 0.704$, $\bar{w} = 0.980$ and $\bar{w}_t = 2.01$. The pulse duration plotted in Fig. 4 is defined by the second moment $[\int t^2|\bar{u}(0,0,z,t)|^2dt/\int|\bar{u}(0,0,z,t)|^2dt]^{1/2}$. For a sech pulse, it is equal to $0.907\bar{w}_t$. The beam width is defined in a similar way. Our simulation is carried out for the nonlinear phase shift up to 32 rad, which should be long enough to verify the existence of spatio-temporal solitary pulses. The accuracy of our numerical simulation is checked by monitoring the pulse energy and the error is found to be of the order of 10^{-5}. From Fig. 4, it can be seen that the solution is stable and behaves almost like real solitons. From Figs. 5 and 6, it can be seen that the pulse shapes during propagation are close to our solution ansatz. The small fluctuations of the pulse parameters in Fig. 4 indicate that the initial pulse parameters and

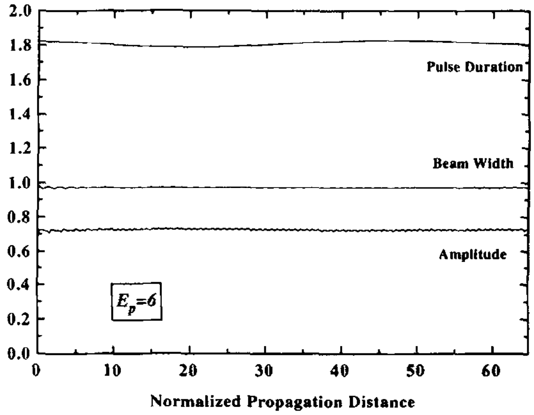

Fig. 4. Amplitude, pulse duration and beam width from numerical simulation for on-axial pulse propagation.

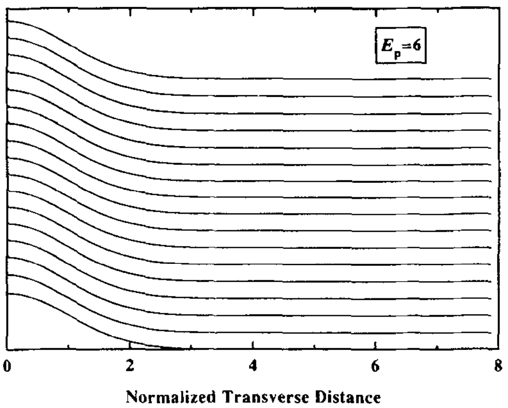

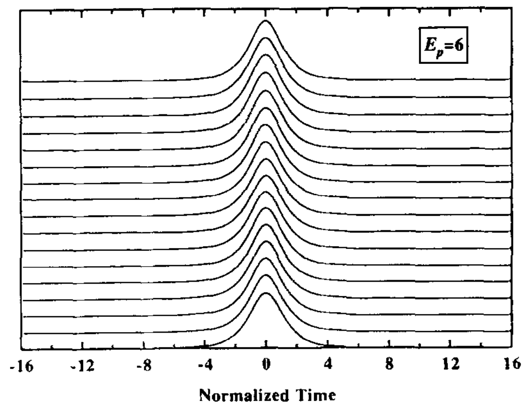

Fig. 5. Spatial pulse shapes sampled for the nonlinear phase shift equal to 0, 2, 4, ..., 32 (from bottom to top).

Fig. 6. Temporal pulse shapes sampled for the nonlinear phase shift equal to 0, 2, 4, ..., 32 (from bottom to top).

pulse shapes we assume are close to but not exactly the real stationary solution. The small mismatch causes the solution to oscillate around the stationary solution. The fluctuations can be reduced by carefully adjusting the input pulse parameters. For smaller pulse energies, the discrepancy between the variational and numerical solutions is smaller. For larger pulse energies, the discrepancy is larger. However, for pulse energies close to the critical energy (i.e. $\bar{E}_p = 12$), the variational solution seems to be unstable, because when the pulse energy is close to the critical energy, the solution ansatz may not be sufficiently accurate. From our calculation, we not only numerically prove the existence of solitary pulses in graded-index Kerr materials but also find that our variational method accurately predicts the pulse parameters of solitary pulses for $\bar{E}_p \leq 10$.

6. Conclusions

We have studied off-axial pulse propagation inside a graded-index waveguide with Kerr nonlinearity. A pulse propagation equation in the time domain, Eq. (7), is derived and used as a starting point for our study. Evolution equations of the pulse parameters are derived using a variational approach, and an approximate analytical expression for the net dispersion parameter is obtained. It is found that our pulse propagation equation is sufficiently accurate for predicting the spatial and temporal evolution when the offset from the optical axis is small. However, it underestimates the net group-velocity dispersion when the offset distance is large. An improved estimation for the net dispersion is derived by taking advantage of the decoupling between the spatial and temporal evolution. It is found that adjustable negative group-velocity dispersion up to 1870 fs^2 can be generated by a 1 cm long commercially available graded-index lens. This makes graded-index waveguides ideal candidates for compact dispersion control elements. In short pulse applications, the Kerr nonlinearity may not be ignored due to the high peak intensity. In the spatial domain, the combined effects of self-focusing and diffraction may exhibit spatial soliton phenomena. Similarly, in the temporal domain, the combined effects of self-phase modulation and negative group-velocity dispersion can also induce temporal soliton phenomena. From our variational approach, we find that in graded-index waveguides with Kerr nonlinearity, the net interaction of self-focusing, diffraction, self-phase modulation, group-velocity dispersion, and graded-index confinement can produce stable spatio-temporal solitary pulses. Their existence criteria and expressions for their pulse parameters are derived. The required negative group-velocity dispersion can be generated by off-axial propagation. From the results obtained, we believe it is not difficult to generate such solitary pulses in a wide range of wavelengths.

In our study of nonlinear pulse propagation in graded-index materials, the major approximation is the solution ansatz, Eq. (18). In particular, in Eq. (18) the beam width is assumed to be the same across the whole pulse. We have verified this assumption by direct numerical simulation for the case of on-axis spatio-temporal solitary pulses propagation. Direct numerical simulation of off-axial solitary pulse propagation will be much more difficult and should be addressed in the future.

Acknowledgements

This research is supported by the National Science Council of ROC under the contract NSC 84-2221-E-009-033. The authors also want to thank the National Center for High-Performance Computing, Republic of China, for offering us their computational power.

References

[1] A.C. Tien, R. Chang and J. Wang, Optics Lett. 17 (1992) 1177.
[2] H.Y. Lin and J. Wang, Measuring geometric group-velocity dispersion in graded-index lenses by spatially coherent white-light interferometry, submitted to the Conference on Lasers and Electro-Optics, Baltimore, Maryland (1995).
[3] R. Chang and J. Wang, Optics Lett. 18 (1993) 266.
[4] Y. Silberberg, Optics Lett. 15 (1990) 1282.
[5] D. Anderson, Phys. Rev. A 15 (1983) 3135.
[6] D. Anderson, M. Lisak and T. Reichel, Phys. Rev. A 38 (1988) 1618.
[7] M. Karlsson, D. Anderson, M. Desaix and M. Lisak, Optics Lett. 16 (1991) 1373.
[8] R.A. Sammut, Q.Y. Li and C. Pask, J. Opt. Soc. Am. B 9 (1992) 884.
[9] R.A. Sammut, C. Pask and Q. Li, J. Opt. Soc. Am. B 10 (1993) 485.
[10] M. Karlsson, D. Anderson and M. Desaix, Optics Lett. 17 (1992) 22.
[11] M. Karlsson and D. Anderson, J. Opt. Soc. Am. B 9 (1992) 1558.
[12] S.-S. Yu, C.-H. Chien, Y. Lai and J. Wang, Optics Comm. 119 (1995) 167.
[13] Y. Chung and N. Dagli, IEEE J. Quantum Electron. 26 (1990) 1335.
[14] W.H. Press, S.A. Teukolsky, W.T. Vetterling and B.P. Flannery, Numerical Recipes: The Art of Scientific Computing, 2nd Ed. (Cambridge Univ. Press, Cambridge, 1992).